

# Force Myography Based Torque Estimation in Human Knee and Ankle Joints

Charlotte Marquardt<sup>\*‡</sup>, Arne Schulz<sup>\*</sup>, Miha Dežman<sup>\*</sup>, Gunther Kurz<sup>†</sup>, Thorsten Stein<sup>†</sup> and Tamim Asfour<sup>\*‡</sup>

**Abstract**—The online adaptation of exoskeleton control based on muscle activity sensing offers a promising approach to personalizing exoskeleton behavior based on the user's biosignals. While electromyography (EMG)-based methods have demonstrated improvements in joint torque estimation, EMG sensors require direct skin contact and extensive post-processing. In contrast, force myography (FMG) measures normal forces resulting from changes in muscle volume due to muscle activity. We propose an FMG-based method to estimate knee and ankle joint torques by integrating joint angles and velocities with muscle activity data. We learn a model for joint torque estimation using Gaussian process regression (GPR). The effectiveness of the proposed FMG-based method is validated on isokinetic motions performed by ten participants. The model is compared to a baseline model that uses only joint angle and velocity, as well as a model augmented by EMG data. The results indicate that incorporating FMG into exoskeleton control can improve the estimation of joint torque for the ankle and knee joints in novel task characteristics within a single participant. Although the findings suggest that this approach may not improve the generalizability of estimates between multiple participants, they highlight the need for further research into its potential applications in exoskeleton control.

## I. INTRODUCTION

Lower limb exoskeletons are wearable devices designed to assist or augment mobility. While their design and control of these devices have traditionally focused on joint biomechanics, there is growing interest in incorporating muscle-level biomechanics to improve the effective interaction with the wearer's musculoskeletal system. Incorporating muscle-level biomechanics into exoskeleton design and control has the potential to overcome some of the current limitations, such as lack of personalization in control strategies, including the need to manually adjust control for each user or track fatigue or energy expenditure [1]. Insights from muscle biomechanics research can enhance understanding of human movement and improve the effectiveness of exoskeleton control [2].

To incorporate muscle biomechanics into exoskeleton control, methods are needed to measure or estimate these biomechanics. Such methods should provide relevant biomechanical data in real-time during static and dynamic motion and must be compatible with the physical structure of the exoskeleton. Electromyography (EMG) is a widely recognized approach to capturing the electrical effects of muscle

activity [3]–[5]. However, ensuring high-quality EMG signals requires extensive filtering and signal post-processing. Several factors can negatively affect signal quality, including electrode positioning on the muscle, electrode skin contact, and electrode displacement during muscle contraction. In contrast, force myography (FMG) detects the mechanical phenomena associated with muscle contraction rather than electrical effects by measuring the normal forces resulting from the muscle volume change. Consequently, it does not require direct skin contact, precise sensor placement on the muscle, and complex post-processing [6], [7]. Since only contact between the body and the exoskeleton is required to measure the interaction forces between both, force sensors can be integrated into exoskeleton cuffs, making FMG-based control of exoskeletons a promising approach.

Estimating human joint torques allows unifying exoskeleton control and thus reduces the user effort [8]. In our previous work, we investigated the use of FMG for exoskeletons using barometric pressure-based FMG units [7], [9]. This paper extends our investigation of using FMG to estimate joint torques of the knee and ankle joint based on the combination of the joint angle and velocity with muscle activity. To do so, we learn a model for joint torque estimation using Gaussian process regression (GPR). We consider the proposed FMG-based approach for estimating joint torque an important initial step towards personalized exoskeleton control. We demonstrate the potential of the approach using data collected in a user study with ten participants performing isokinetic exercises, in which the velocity of the limb movement is maintained constant with varying resistance and muscle forces. To evaluate the FMG-based approach, we compared our model to a baseline model that only uses joint angle and velocity, as well as a model augmented by EMG data (Fig. 1).

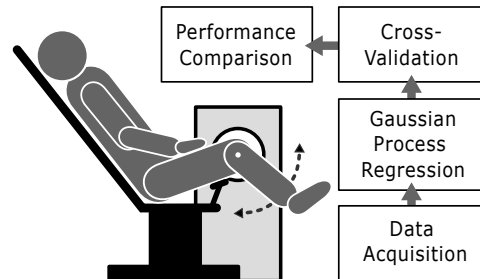


Fig. 1: Schematic overview of the process of data acquisition, regression, and evaluation.

This work has been supported by the Carl Zeiss Foundation through the JuBot project and the German Federal Ministry of Education and Research (BMBF) under the Robotics Institute Germany (RIG).

<sup>\*</sup>High Performance Humanoid Technologies Lab, Institute for Anthropomatics and Robotics, Karlsruhe Institute of Technology (KIT), Germany

<sup>†</sup>BioMotion Center, Institute of Sports and Sports Sciences, Karlsruhe Institute of Technology (KIT), Germany

<sup>‡</sup> Corresponding authors: {charlotte.marquardt, asfour}@kit.edu

The paper is organized as follows. Section II discusses current related work while Section III describes the model used to estimate the joint torques, the user study conducted, the sensor setup used, and the processing of the recorded signals. The quality of the torque estimation and its validation results are presented in Section IV and discussed in Section V. Section VI concludes the paper.

## II. RELATED WORK

The introduction of joint torque estimation in exoskeleton control aims to provide momentous feedback in a closed-loop control system. This enables task-independent control, eliminating the need for discretization of human motion, resulting in task-dependent feedforward control trajectories [8]. Using multiple sensing methods to capture muscle activity has created an opportunity to optimize human joint torque estimation during exoskeleton usage. Previous work has explored a variety of EMG-driven methods for actuation and estimation of joint torques in exoskeleton control, and intention prediction.

EMG methods combined with neuromusculoskeletal (NMS) models enhance human-robot cooperation in exoskeletons by considering joint angles and muscle dynamics [10], [11]. This combination performs best during high muscle activation trials, but pairing it with artificial neural network (ANN) showed superior performance with diverse training data [12]. Recent hybrid NMS models combined with ANN and convolutional neural network (CNN) have been shown to outperform traditional NMS models in torque estimation [13], [14]. Additionally, combining inertial sensors with EMG-driven simulations supports the characterization of knee joint mechanics during walking [15], [16], while NMS models have been shown to enable personalized torque estimations in the ankle joint using real-time EMG data [17]. Other EMG-based methods use deep learning methods [18]–[20], such as temporal convolutional networks (TCNs) [21], CNN [14] or ANN [13] directly to estimate lower limb joint torques and optimize its performance. Although these methods surpass traditional NMS models, their effectiveness in a hybrid model with NMS varies based on the specific model and application [13], [14]. Proportional myoelectric control directly uses the muscle activity amplitude to control the torque output of the exoskeleton [22]. Studies showed that users of a proportional myoelectric controlled ankle exoskeleton maintained their normal joint biomechanics [23], however, the effect on metabolic cost was limited during walking both on a treadmill and outdoors [24], [25]. Moreover, these controllers measure only the resulting behavior of the muscle actions and thus do not fully capture the muscle and body mechanics [1]. In general, these results show the potential to integrate EMG signals, either directly or in advanced algorithms, to personalize joint torque estimation and torque control of exoskeletons.

On the other hand, FMG signals have been extensively and successfully investigated in various wearable applications such as upper arm or hand motion classification and intention detection [26]–[29], lower limb gait phase or event

detection [30], [31] and ankle position classification [32] often showing to outperform EMG-based methods. Research indicates a nonlinear relationship between muscle surface deformation and torque, implying that muscle deformation could be an effective signal for non-invasive, real-time torque measurement [33]. Sakr et al. [34] demonstrated promising results of using FMG signals from the lower arm to estimate multi-directional isometric hand force/torque. The feasibility of estimating lower-limb joint torques using FMG signals has yet to be investigated and compared to methods based on EMG and kinematic sensors alone.

## III. METHODS

Accurate biomechanical models of joint kinematics in combination with normal muscle forces are difficult to obtain. To learn the relationship between kinematics and muscle force, we propose a GPR model. This section describes the model and the user study, including the sensor setup used to provide data for the training and validation of the model. A schematic overview of the entire torque estimation and validation process is given in Fig. 2.

### A. Joint Torque Estimation Model

GPR models are a kernel-based probabilistic and parametric supervised learning method for input-output mapping of empirical data that follows a joint Gaussian distribution [35]. In vector form, this can be expressed by

$$f(\mathbf{x}) \sim \mathcal{GP}(m(\mathbf{x}), k(\mathbf{x}, \mathbf{x}')), \quad (1)$$

where an observed outcome  $f(\mathbf{x})$  is estimated from an input  $\mathbf{x}$  by a Gaussian process with the mean function  $m$  and the covariance function  $k(\mathbf{x}, \mathbf{x}')$ . For the covariance function, the radial basis function (RBF)

$$k(\mathbf{x}, \mathbf{x}') = \sigma^2 \exp\left(-\frac{|\mathbf{x} - \mathbf{x}'|^2}{2l^2}\right), \quad (2)$$

with the length scale  $l$  and the error variance  $\sigma^2$  was chosen. These hyperparameters are optimized with the mean function, maximizing the log marginal likelihood and minimizing the cross-validation loss. The mean function is often used to incorporate prior knowledge and is commonly set to zero if no approximation model is known.

The input  $\mathbf{x}$  is defined for three different configurations:

$$\mathbf{x} = \begin{cases} (\theta_J, \omega_J)^T & \text{baseline} \\ (\theta_J, \omega_J, \mathbf{M}_{\text{EMG}})^T & \text{EMG} \\ (\theta_J, \omega_J, \mathbf{M}_{\text{FMG}})^T & \text{FMG} \end{cases} \quad (3)$$

where  $\theta_J$  represents the joint angle,  $\omega_J$  the joint angular velocity, and  $\mathbf{M}$  the muscle signals obtained either from FMG or EMG signals. These result in the corresponding estimated joint torques  $\tilde{T}_{J,\text{baseline}}$ ,  $\tilde{T}_{J,\text{FMG}}$  and  $\tilde{T}_{J,\text{EMG}}$ .

For each joint, the muscle signal  $\mathbf{M}$  was selected based on the primary muscles involved in the motion of that joint [36]:

$$\mathbf{M} = \begin{cases} (M_{\text{TA}}, M_{\text{GM}}, M_{\text{GL}}) & \text{ankle joint} \\ (M_{\text{BF}}, M_{\text{RF}}, M_{\text{ST}}, M_{\text{VM}}, M_{\text{VL}}) & \text{knee joint} \end{cases} \quad (4)$$

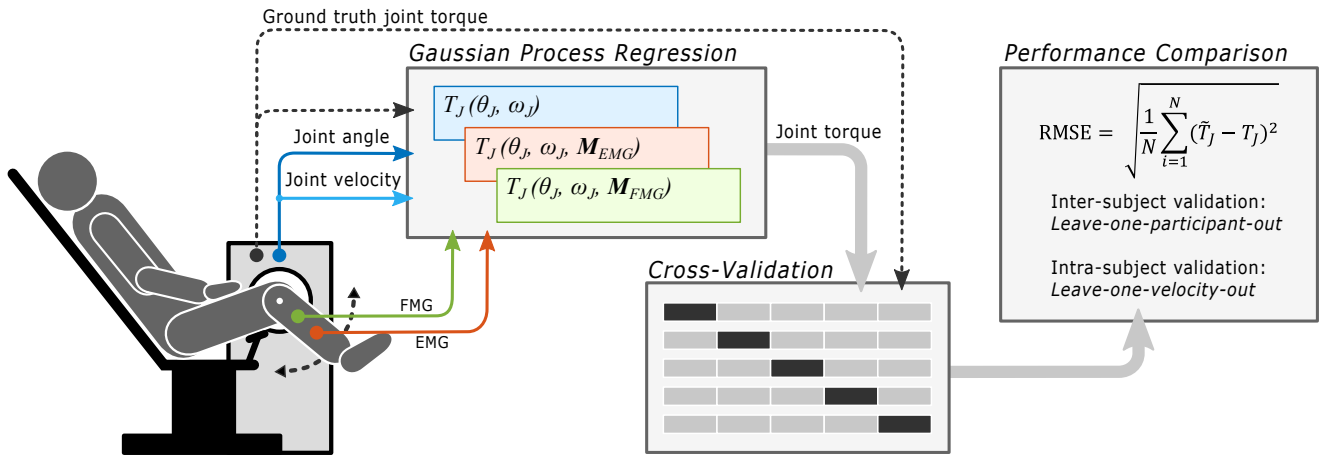


Fig. 2: Schematic representation of the torque estimation and validation process for knee joint motion.

where  $M_{TA}$ ,  $M_{GM}$ ,  $M_{GL}$ ,  $M_{BF}$ ,  $M_{RF}$ ,  $M_{ST}$ ,  $M_{VM}$  and  $M_{VL}$  correspond to the muscular signals of the *tibialis anterior* (TA), *gastrocnemius medialis* (GM), *gastrocnemius lateralis* (GL), *biceps femoris* (BF), *rectus femoris* (RF), *semitendinosus* (ST), *vastus medialis* (VM) and *vastus lateralis* (VL). The effects of biarticular muscles, which influence the movements of multiple joints at the same time, have not been considered beyond the joints described in Eq. (4).

### B. User Study

To validate the model combining joint biomechanics and muscle signals in isokinetic motion, a user study was carried out in a controlled laboratory environment using an IsoMed 2000 device. This device includes an integrated mode that facilitates isokinetic movement of a single joint at a time (Fig. 3) and offers a direct on-axis measurement of the true sagittal joint torque. During isokinetic movement, the velocity of limb motion remains constant while the muscle forces can change. This provides a controlled experimental setup with minimal disturbances or external forces acting on the sensors during the motion.

In the study, ten healthy, able-bodied adults participated ( $m = 5 \mid f = 5$ , age  $26.8 \pm 3.2$  years, height  $175.2 \pm 6.78$  cm, weight  $65.0 \pm 6.8$  kg). The experimental protocol was approved by the Karlsruhe Institute of Technology (KIT) Ethics Committee under the JuBot project. Participants provided their informed consent in writing prior to the experiment, and all methods were performed following the Declaration of Helsinki.

The experiment was conducted with participants positioned on the IsoMed device, where their left leg was secured on either a foot or shank support. This arrangement permitted pure sagittal movement of the ankle or knee joint as shown in Fig. 3. Participants were given up to 10 min to familiarize themselves with the IsoMed device, during which the device's rotation axis was carefully aligned with the sagittal axis of rotation of the joint using a built-in laser pointer. Furthermore, the mechanical end stops of the device were positioned to correspond to the user's maximum range

of motion (RoM) within their anatomical limits. Following this, the participants performed two tasks in a random order:

- *Knee*: First, the knee joint was positioned at the maximum extension for initialization (Fig. 3a). Next, the participant performed a series of five swing motions, including flexion and extension within their maximum active range of motion, maintaining a constant maximum angular velocity. These motions were carried out at four different angular velocities:  $60^\circ/s$ ,  $90^\circ/s$ ,  $120^\circ/s$ , and  $150^\circ/s$ . The initialization procedure and the five swing motions were repeated three times for each velocity, resulting in three recordings per angular velocity.
- *Ankle*: The ankle joint was first initialized in a position in which the foot was orthogonal to the shank (Fig. 3b). Next, the participant performed five swing motions, including dorsi- and plantarflexion between the maximum angles of their active joint range. The initialization procedure and the five swing motions were repeated three times for velocities:  $30^\circ/s$ ,  $60^\circ/s$ ,  $90^\circ/s$  and  $120^\circ/s$ , resulting in three recordings per angular velocity.

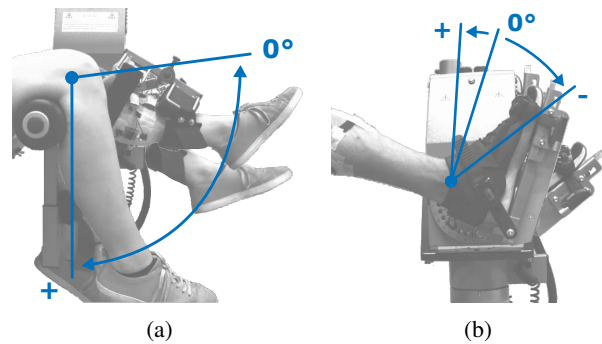


Fig. 3: participant set-up on the IsoMed system for knee motion (a) and ankle motion (b) and the corresponding definition of the direction of the joint angle  $\theta_J$ .

For calibration purposes, the FMG sensors were initialized before accessing the IsoMed device by standing upright and relaxed on both feet for approximately 10 seconds. Calibration measurements of the joint angle were conducted at each initial position  $\theta_j = 0^\circ$  as marked in Fig. 3.

### C. Sensor Setup

The used FMG sensor unit measures the normal force resulting from a change in volume and stiffness of the human muscle underneath the cuff during leg motion. The sensor unit comprises five barometric pressure sensors on a single printed circuit board (PCB), covered by a silicon dome. Variations in pressure detected by these sensors reflect changes in the forces applied to the silicon dome. A detailed description of the sensor unit is given in [7],

In our experiments, eight FMG units and eight EMG electrode pairs were placed at anatomically relevant locations to measure the muscle activity of *RF*, *BF*, *ST*, *VM*, *VL*, *GM*, *GL* and *TA* as displayed in Fig. 4. The positions were determined based on EMG placement recommendations given in SENIAM [37] combined with an assessment of real-time feedback of the EMG sensor. The two EMG electrodes were attached above and below the FMG sensor unit along the course of the muscle to ensure measurement at the same point on the muscle. In addition, the respective angular position  $\theta_j$  and torque of the joints  $T_j$  were recorded via the IsoMed device.

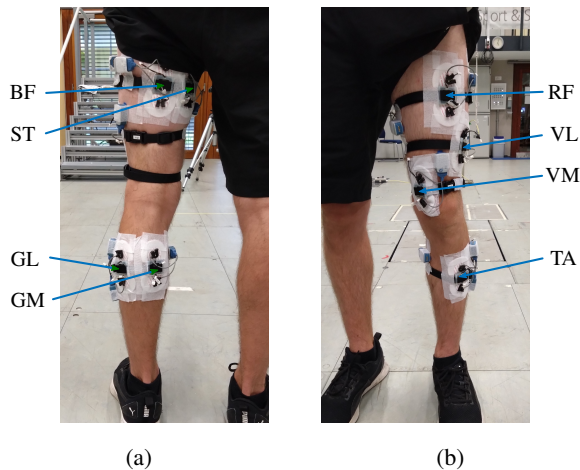


Fig. 4: EMG (white electrodes) and FMG (black straps) sensor positions on the back (a) and front (b) of the left leg.

### D. Signal Processing

The amplitudes of the EMG signals are stochastic, and the signal fluctuates rapidly around zero. Therefore, the signals were band-pass filtered between 20 Hz to 500 Hz, rectified and afterwards low-pass filtered at 6 Hz. Both filters applied were fourth-order bi-directional Butterworth filters to achieve zero phase distortion. The baseline offset was removed using the mean values obtained from the calibration measurements

to calibrate both the FMG signal and the joint angle signal. No further filtering was applied to the FMG signal.

The angular joint velocity was derived based on the joint angle measurements. A second-order Butterworth filter with a cutoff frequency of 20 Hz was applied bi-directionally before calculating the gradient. The segmentation of each complete motion, including flexion and extension of the knee joint and dorsi- and plantarflexion of the ankle joint, was performed based on the filtered joint angle to make it easier to recognize their extrema corresponding to the change in direction.

The FMG sensor units allow a maximum sampling rate of 200 Hz, while the joint angle, joint torque, and EMG signals were sampled at 2000 Hz. To align and concatenate all data, each dataset was linearly interpolated to an equidistant number of data points, resulting in a down-sampling of the joint angle and EMG data to fit the FMG data. To ensure that the data can be easily compared, all values were standardized using Z-score normalization, and after regression, the estimated joint torque was denormalized to its original scale.

To compare both the inter- and intra-participant performance of the model, the evaluation of the estimation results was based on a leave-one-participant-out (LOPO) and a leave-one-velocity-out (LOVO) cross-validation. The LOPO method integrates the concatenated data of all four velocities for each participant, and the LOVO is performed separately for each participant. Since the computational complexity of GPR is  $O(n^3)$ , a sparse gaussian process regression (SGPR) was used to train the model for LOPO. The initial inducing points are a randomly selected subset of 0.25 % and 10 % of the training data for LOPO and LOVO, respectively. Early stopping was used with a patience of 50 epochs to avoid overfitting, tracking the validation loss based on 20 % of the training data, and restoring the best model if no improvement was made over these 50 epochs.

The standard deviation of the model estimation was evaluated by root-mean-squared error (RMSE). A lower value of RMSE implies a higher accuracy of the GPR model. Model training and testing were done using TensorFlow.

## IV. RESULTS AND ANALYSIS

The proposed GPR-based joint torque estimation approach was evaluated using LOPO and LOVO cross-validations to assess its performance. The RMSE values from these validations are presented in Fig. 5 for both the ankle and knee joints and the three model configurations. The performance of the approaches varies between the LOPO and LOVO validations. In the LOPO validation, the RMSE values indicate that the baseline model is the most accurate of the three approaches. Conversely, the LOVO validation shows that the extended model with FMG signals achieves comparable or better performance than the baseline model. In the LOPO validation, the EMG-based model outperforms the FMG-based model for most participants but performs worse in the LOVO validation. However, the LOPO results indicate that the FMG-based model performs better for the knee joint than

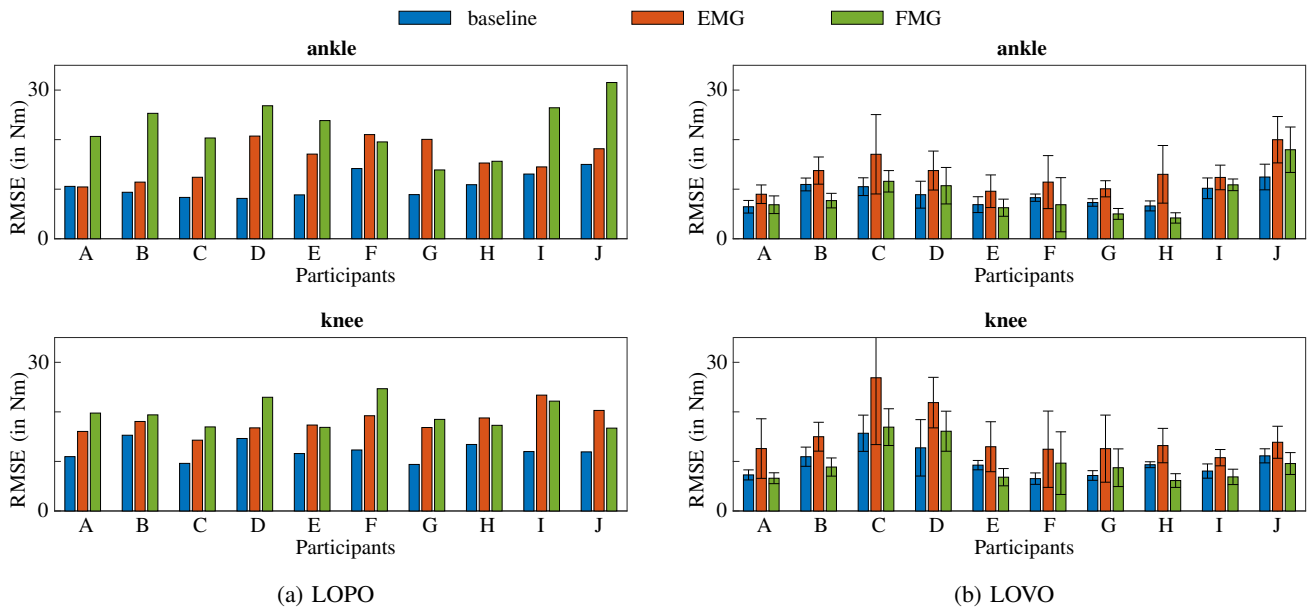


Fig. 5: RMSE of the LOPO (a) and mean and standard deviation of the RMSE over all four velocities of the LOVO (b) validation for all three model configurations, baseline (blue, left), EMG (orange, middle) and FMG (green, right) of both the ankle (top) and knee (bottom) joint.

for the ankle joint, outperforming the EMG-based model for four participants.

Figure 6 presents an example of joint torque estimation from time series data of a single participant, comparing estimated and measured joint torque during isokinetic motion at  $60^\circ/s$  based on the corresponding test data. The baseline model, which considers only joint angle and velocity, pro-

vides a stable estimate but fails to capture the variations in the true torque amplitude. In contrast, incorporating muscle signals improves the model’s ability to capture the variations in true torque amplitude that vary across participants and speeds. However, this also results in greater variability compared to true torque amplitude in the EMG or FMG based torque estimates for LOVO and LOPO, respectively.

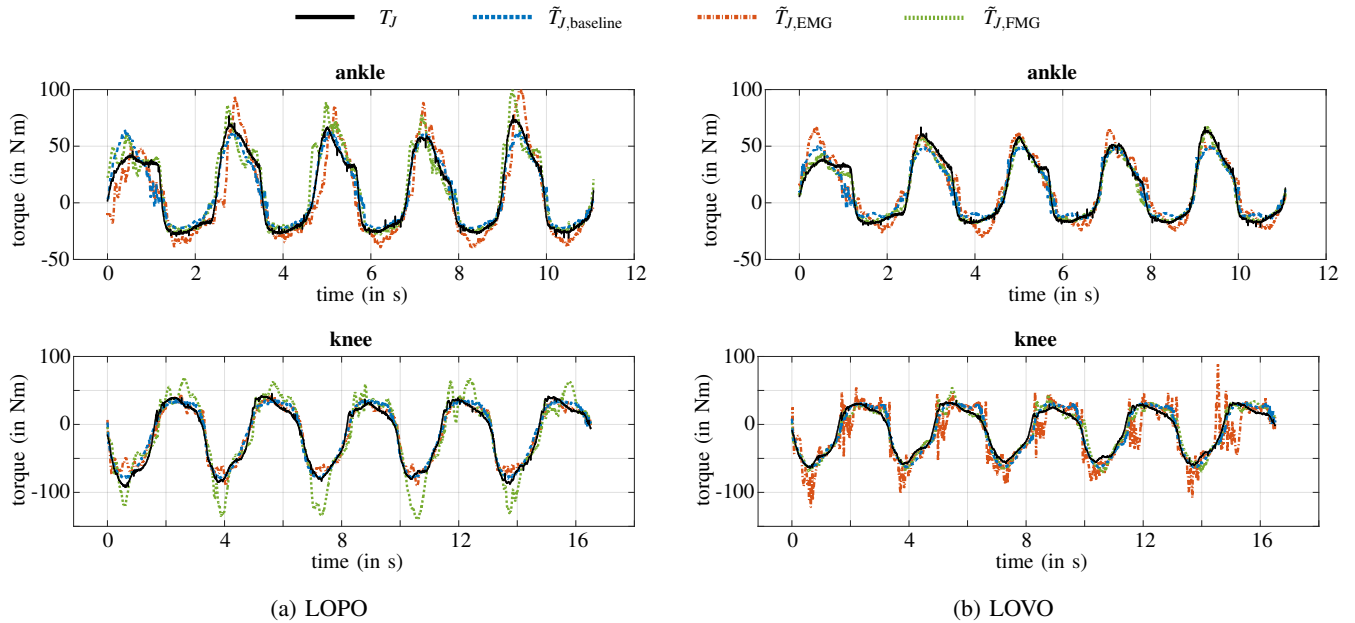


Fig. 6: Measured and estimated torque over time for all three model configurations, baseline (blue, dashed), EMG (orange, dash-dotted) and FMG (green, dotted) of both the ankle (top) and knee (bottom) joint. The exemplary data of (a) the LOPO and (b) the LOVO validation is based on the testing data of one recording of the isokinetic motion of participant G at  $60^\circ/s$ .

## V. DISCUSSION

This work presents a FMG-based approach to estimating torques in the knee and ankle joints. It uses joint angles and velocities together with muscle activity in a GPR. The effectiveness of this FMG-based method is validated through a study with ten participants and compared to a baseline model using only joint angle and velocity, as well as a model based on EMG.

The LOPO validation showed that a model based on joint angle and velocity is more effective for generalization across multiple users, including novel ones. This observation may be due to the comprehensive recording of the full range of motion in each experiment, resulting in joint angle and velocity data that are more consistent across participants. In contrast, muscle activity is influenced by factors such as varying fitness levels and fatigue, resulting in fluctuations in amplitudes even after calibration. The results suggest that the electrical activation of muscles tends to be more uniform across individuals, as shown by the similar RMSE of the EMG signals in the LOPO validation. In contrast, the RMSE of the LOPO validation suggests that the volume of muscle activity itself is less consistent across individuals. These results may be attributed to the validation of isokinetic motion focused on the sagittal plane. Previous research has shown that the integration of muscle activity into joint torque estimation models is more advantageous for non-cyclic than for cyclic tasks [21]. Therefore, future research will include a range of activities of daily living to confirm the findings across a spectrum of combined motions and to determine the comprehensibility of muscular signals during motions, including multidirectional and non-periodic motions.

The integration of muscle activity into the joint torque estimation appears to improve generalization to novel task characteristics, such as changes in task velocity and variations in the torque amplitude. This is reflected in the low RMSE values observed in the LOVO validation for several participants and is supported by the visualization of the corresponding torque trajectories of the five exemplary swings. In this context, the estimation based on FMG demonstrates greater accuracy than the EMG-based model, which is almost comparable to the baseline model. Belyea et al. [29] reported similar findings in their study of human wrist motion utilizing support vector regression (SVR).

The proposed GPR model uses a fully data-driven approach with a difficult-to-interpret model. Future research will aim to integrate additional prior knowledge into the GPR model, drawing inspiration from biomechanical models or exploring other more interpretable model alternatives. This has the potential to reduce the data requirements for model training and provide a clearer understanding of how each input signal influences the model output. In addition, it may be possible to distinguish between a generalizable model based on joint angles and velocities and a customizable model based on muscle activity. This separation could allow the general model to be optimized for each individual during use. In contrast, less comprehensive and more data-driven

models such as ANN [12] and CNN [14] have so far proven to be well suited for EMG-based joint torque estimation in isokinetic and non-weight-bearing applications as well as during walking.

In the future, when using an exoskeleton, it is expected that the forces used to move the exoskeleton may interfere with the measurement of muscle activity using FMG due to potential disturbance forces caused by the interaction between the exoskeleton and the user. Even within this laboratory setup, it remains a challenge to eliminate the possibility that other parasitic forces - arising from co-contraction or external perturbations - may interfere with FMG measurements. The decision to use the IsoMed device was aimed at mitigating the influence of as many parasitic forces as possible. In our previous work, we have shown how motion restrictions due to an ankle exoskeleton can affect FMG sensor signals [9]. Further research will reveal the extent to which actuation can affect FMG-based torque estimation and control.

The results emphasize that FMG technology offers a promising alternative to EMG technology for the development of a more personalized assistive exoskeleton, but further research on its performance and applicability in exoskeleton control is needed.

## VI. CONCLUSION

Incorporating muscle activity signals is a promising approach for online personalization of exoskeleton control. In this work, we proposed an FMG-based approach to estimate knee and ankle joint torques using joint angles, velocities, and muscle activity in a GPR model. To validate the effectiveness of FMG-based torque estimation, we conducted a user study with ten subjects performing isokinetic ankle and knee motion. A comparative analysis was performed against a baseline model using only joint angle and velocity data, and a model augmented with muscle activity signals obtained from EMG sensors. The results reveal that incorporating FMG data into the exoskeleton control improves the estimation of joint torque for the ankle and knee joints in the presence of unknown task characteristics, such as velocity changes, for each subject. While the results may not show improved generalizability across different subjects, the findings underscore the need for further research into the potential of FMG as an alternative to EMG for developing control strategies for exoskeletons.

## ACKNOWLEDGMENT

The authors would like to thank Tim Wolk (High Performance Humanoid Technologies Lab, Karlsruhe Institute of Technology (KIT)) for his support in facilitating training and testing on multiple participants.

## REFERENCES

- [1] Z. S. Mahdian, H. Wang, M. I. M. Refai, G. Durandau, M. Sartori, and M. K. MacLean, "Tapping Into Skeletal Muscle Biomechanics for Design and Control of Lower Limb Exoskeletons: A Narrative Review," *Journal of Applied Biomechanics*, vol. 39, no. 5, pp. 318–333, 2023.
- [2] J. Wang, D. Wu, Y. Gao, X. Wang, X. Li, G. Xu, and W. Dong, "Integral Real-time Locomotion Mode Recognition Based on GA-CNN for Lower Limb Exoskeleton," *Journal of Bionic Engineering*, Jul. 2022.
- [3] C. D. Joshi, U. Lahiri, and N. V. Thakor, "Classification of gait phases from lower limb EMG: Application to exoskeleton orthosis," in *2013 IEEE Point-of-Care Healthcare Technologies (PHT)*, Jan. 2013, pp. 228–231, iSSN: 2377-5270.
- [4] J. Taborri, E. Palermo, S. Rossi, and P. Cappa, "Gait Partitioning Methods: A Systematic Review," *Sensors*, vol. 16, no. 1, 2016.
- [5] S. Jiang, P. Kang, X. Song, B. Lo, and P. B. Shull, "Emerging Wearable Interfaces and Algorithms for Hand Gesture Recognition: A Survey," *IEEE Reviews in Biomedical Engineering*, pp. 1–1, 2021.
- [6] C. Castellini and V. Ravindra, "A wearable low-cost device based upon Force-Sensing Resistors to detect single-finger forces," in *5th IEEE RAS/EMBS International Conference on Biomedical Robotics and Biomechanics*. Sao Paulo, Brazil: IEEE, Aug. 2014, pp. 199–203.
- [7] C. Marquardt, P. Weiner, M. Dežman, and T. Asfour, "Embedded barometric pressure sensor unit for force myography in exoskeletons," in *IEEE/RAS International Conference on Humanoid Robots (Humanoids)*, Ginowan, Okinawa, Japan, 2022, pp. 67–73.
- [8] D. D. Molinaro, I. Kang, and A. J. Young, "Estimating human joint moments unifies exoskeleton control, reducing user effort," *Science Robotics*, vol. 9, no. 88, p. eadi8852, Mar. 2024.
- [9] C. Marquardt, M. Dežman, and T. Asfour, "Influence of motion restrictions in an ankle exoskeleton on force myography in straight and curve walking," in *IEEE/RAS/EMBS International Conference on Biomedical Robotics and Biomechanics (BioRob)*, Heidelberg, Germany, September 2024.
- [10] D. Ao, R. Song, and J. Gao, "Movement Performance of Human-Robot Cooperation Control Based on EMG-Driven Hill-Type and Proportional Models for an Ankle Power-Assist Exoskeleton Robot," *IEEE Transactions on Neural Systems and Rehabilitation Engineering*, vol. 25, no. 8, pp. 1125–1134, Aug. 2017.
- [11] D. Xu, Q. Wu, and Y. Zhu, "Development of a sEMG-Based Joint Torque Estimation Strategy Using Hill-Type Muscle Model and Neural Network," *Journal of Medical and Biological Engineering*, vol. 41, no. 1, pp. 34–44, Feb. 2021.
- [12] L. Zhang, Z. Li, Y. Hu, C. Smith, E. M. G. Farewik, and R. Wang, "Ankle Joint Torque Estimation Using an EMG-Driven Neuromusculoskeletal Model and an Artificial Neural Network Model," *IEEE Transactions on Automation Science and Engineering*, vol. 18, no. 2, pp. 564–573, Apr. 2021.
- [13] L. Zhang, X. Zhu, E. M. Gutierrez-Farewik, and R. Wang, "Ankle Joint Torque Prediction Using an NMS Solver Informed-ANN Model and Transfer Learning," *IEEE Journal of Biomedical and Health Informatics*, vol. 26, no. 12, pp. 5895–5906, Dec. 2022.
- [14] R. V. Schulte, M. Zondag, J. H. Buurke, and E. C. Prinsen, "Multi-Day EMG-Based Knee Joint Torque Estimation Using Hybrid Neuromusculoskeletal Modelling and Convolutional Neural Networks," *Frontiers in Robotics and AI*, vol. 9, p. 869476, Apr. 2022.
- [15] R. D. Gurchiek, N. Cheney, and R. S. McGinnis, "Estimating Biomechanical Time-Series with Wearable Sensors: A Systematic Review of Machine Learning Techniques," *Sensors*, vol. 19, no. 23, p. 5227, Nov. 2019.
- [16] R. D. Gurchiek, N. Donahue, N. M. Fiorentino, and R. S. McGinnis, "Wearables-Only Analysis of Muscle and Joint Mechanics: An EMG-Driven Approach," *IEEE Transactions on Biomedical Engineering*, vol. 69, no. 2, pp. 580–589, Feb. 2022.
- [17] G. Durandau, W. F. Rampeltshammer, H. v. d. Kooij, and M. Sartori, "Neuromechanical Model-Based Adaptive Control of Bilateral Ankle Exoskeletons: Biological Joint Torque and Electromyogram Reduction Across Walking Conditions," *IEEE Transactions on Robotics*, vol. 38, no. 3, pp. 1380–1394, Jun. 2022.
- [18] M. E. Hahn and K. B. O'Keefe, "A Neural Network Model For Estimation Of Net Joint Moments During Normal Gait," *Journal of Musculoskeletal Research*, vol. 11, no. 03, pp. 117–126, Sep. 2008.
- [19] H. C. Siu, J. Sloboda, R. J. McKindles, and L. A. Stirling, "A Neural Network Estimation of Ankle Torques From Electromyography and Accelerometry," *IEEE Transactions on Neural Systems and Rehabilitation Engineering*, vol. 29, pp. 1624–1633, 2021.
- [20] J. Camargo, D. Molinaro, and A. Young, "Predicting biological joint moment during multiple ambulation tasks," *Journal of Biomechanics*, vol. 134, p. 111020, Mar. 2022.
- [21] K. L. Scherpereel, D. D. Molinaro, M. K. Shepherd, O. T. Inan, and A. J. Young, "Improving Biological Joint Moment Estimation During Real-World Tasks With EMG and Instrumented Insoles," *IEEE Transactions on Biomedical Engineering*, vol. 71, no. 9, pp. 2718–2727, Sep. 2024.
- [22] R. L. Hybart and D. P. Ferris, "Preliminary Validation of Proportional Myoelectric Control of A Commercially Available Robotic Ankle Exoskeleton," in *2022 International Conference on Rehabilitation Robotics (ICORR)*. Rotterdam, Netherlands: IEEE, Jul. 2022, pp. 1–5.
- [23] —, "Neuromechanical Adaptation to Walking With Electromechanical Ankle Exoskeletons Under Proportional Myoelectric Control," *IEEE Open Journal of Engineering in Medicine and Biology*, vol. 4, pp. 119–128, 2023.
- [24] R. Hybart, K. S. Villancio-Wolter, and D. P. Ferris, "Metabolic cost of walking with electromechanical ankle exoskeletons under proportional myoelectric control on a treadmill and outdoors," *PeerJ*, vol. 11, p. e15775, Jul. 2023.
- [25] R. Hybart and D. Ferris, "Gait variability of outdoor vs treadmill walking with bilateral robotic ankle exoskeletons under proportional myoelectric control," *PLOS ONE*, vol. 18, no. 11, p. e0294241, Nov. 2023.
- [26] M. R. U. Islam and S. Bai, "Effective Multi-Mode Grasping Assistance Control of a Soft Hand Exoskeleton Using Force Myography," *Frontiers in Robotics and AI*, vol. 7, p. 139, 2020.
- [27] Z. G. Xiao and C. Menon, "Performance of forearm FMG and sEMG for estimating elbow, forearm and wrist positions," *Journal of Bionic Engineering*, vol. 14, no. 2, pp. 284–295, 2017.
- [28] X. Jiang, L.-K. Merhi, Z. G. Xiao, and C. Menon, "Exploration of Force Myography and surface Electromyography in hand gesture classification," *Medical Engineering & Physics*, vol. 41, pp. 63–73, Mar. 2017.
- [29] A. Belyea, K. Englehart, and E. Scheme, "FMG Versus EMG: A Comparison of Usability for Real-Time Pattern Recognition Based Control," *IEEE Transactions on Biomedical Engineering*, vol. 66, no. 11, pp. 3098–3104, Nov. 2019.
- [30] M. R. Islam and S. Bai, "A novel approach of FMG sensors distribution leading to subject independent approach for effective and efficient detection of forearm dynamic movements," *Biomedical Engineering Advances*, vol. 4, p. 100062, 2022.
- [31] X. Jiang, H. T. Chu, Z. G. Xiao, L.-K. Merhi, and C. Menon, "Ankle positions classification using force myography: An exploratory investigation," in *2016 IEEE Healthcare Innovation Point-Of-Care Technologies Conference (HI-POCT)*, Nov. 2016, pp. 29–32.
- [32] X. Jiang, L. Tory, M. Khoshnam, K. Chu, and C. Menon, "Exploration of Gait Parameters Affecting the Accuracy of Force Myography-Based Gait Phase Detection," in *2018 7th IEEE International Conference on Biomedical Robotics and Biomechanics (Biorob)*, Aug. 2018, pp. 1205–1210, iSSN: 2155-1782.
- [33] J. T. Alvarez, A. De Marcillac, Y. Jin, L. F. Gerez, O. A. Araromi, and C. J. Walsh, "Surface-Level Muscle Deformation as a Correlate for Joint Torque," *Advanced Materials Technologies*, p. 2400444, May 2024.
- [34] M. Sakr, X. Jiang, and C. Menon, "Estimation of User-Applied Isometric Force/Torque Using Upper Extremity Force Myography," *Frontiers in Robotics and AI*, vol. 6, p. 120, Nov. 2019.
- [35] C. E. Rasmussen and Christopher K. I. Williams, *Gaussian process for machine learning*. London, England: The MIT Press, 2006, oCLC: 999818656.
- [36] D. A. Neumann and E. E. Rowan, *Kinesiology of the musculoskeletal system: foundations for physical rehabilitation*, 1st ed. St. Louis: Mosby, 2002, oCLC: 992214437.
- [37] H. J. Hermens, B. Freriks, R. Merletti, D. Stegeman, J. Blok, G. Rau, C. Disselhorst-Klug, and G. Hägg, "Seniam," 1999, publisher: Roessingh Research and Development. [Online]. Available: <http://seniam.org/>